JCTC Journal of Chemical Theory and Computation

Car–Parrinello Molecular Dynamics Simulations of $CaCl_2$ Aqueous Solutions

Teodora Todorova,[†,‡] Philippe H. Hünenberger,[§] and Jürg Hutter*[,†]

Physical Chemistry Institute, University of Zurich, CH-8057 Zurich, Switzerland, and Laboratory for Physical Chemistry, Swiss Federal Institute of Technology (ETH), CH-8093 Zurich, Switzerland

Received November 7, 2007

Abstract: Car–Parrinello molecular dynamics (CPMD) simulations are used to investigate the structural properties of 1 and 2 molal (m) $CaCl_2$ aqueous solutions and, in particular, the radial distribution functions, coordination numbers, and dipole moments of water molecules in the first solvation shell. According to these simulations, the first solvation shell of the Ca^{2+} ion consists of six water molecules, that are characterized by an increased averaged dipole moment compared to that of bulk water, and a first-shell Ca−O radial distribution function peak at 2.39 Å. The results are compared to those of CPMD simulations of Ca^{2+} (no counterions), and no significant differences are found. This indicates that the homogeneous neutralizing background charge density implicitly included in simulations of non-neutral systems appropriately mimics the presence of the counterions (at least in terms of reproducing the solvation structure properties and for the box sizes considered). Classical molecular dynamics (MD) simulations of aqueous Ca^{2+} using varying box sizes confirm this suggestion. The CPMD simulations at 2 m concentration also reveal additional possibilities for the structural arrangement of water molecules and chloride ions around Ca^{2+}. In particular, they support the stability of Ca^{2+}-Cl^- (contact) and Ca^{2+}-H_2O-Cl^- (solvent-separated) ion pairs. In addition, the solvent-separated cation pair is found to occur in a deprotonated Ca^{2+}-OH^--Ca^{2+} form. The existence of such a species has, to our knowledge, never been invoked previously to account for experimental data on $CaCl_2$ solutions.

1. Introduction

Although the Ca^{2+} aqua-ion is of great importance in biology and a key component of natural ground waters, many details of its solvation structure remain controversial.[1] Even for such fundamental properties as the average coordination number (CN) and the average Ca−O distance (r[Ca−O]) for the first solvation shell, the results widely depend on the (experimental or theoretical) method of investigation. Challenges to experimental approaches involve factors such as the low atomic number of the element (relatively weak scattering center) and the uncertainty in modeling the scattering data (solute–solvent correlations only accounting for a very limited fraction of the measured scattering intensities). In addition the r[Ca−O] distance of about 2.5 Å leads to a partial occlusion of the corresponding peak by the broad O−O peak of water in diffraction studies, rendering the experimental determination of the hydration structure difficult, in particular in the dilute regime. Based on X-ray diffraction (XRD) experiments on aqueous solutions of calcium halides or nitrate, CNs ranging between 5.9 and 8 have been reported[2–8] at concentrations ranging (in molal units) between 1 and 6 m (Table 1). Neutron diffraction (ND) experiments yielded values ranging between 5.5 and 10 in the concentration range between 1 and 6.4 m.[7,9–11] Extended X-ray absorption fine structure (EXAFS) measurements resulted in CNs between 6.8 and 8[12,13] at concentrations ranging from 0.12 to 6 m. Recently, Megyes et al.[7] reported the results of combined XRD and ND experiments on 2.5

* Corresponding author. E-mail: hutter@pci.uzh.ch.
† University of Zurich.
‡ Current address: Paul-Scherrer-Institute (PSI), 5232 Villigen, Switzerland.
§ Swiss Federal Institute of Technology (ETH).

10.1021/ct700302m CCC: $40.75
Published on Web 04/15/2008

Table 1. Experimental Results on Ca^{2+} Solvation Previously Reported in the Literature Based on X-ray Diffraction (XRD), Neutron Diffraction (ND), and Extended X-ray Absorption Fine Structure (EXAFS) Studies[a]

ref	method	salt	concn (m)	CN	r[Ca−O] (Å)
2	XRD	$CaCl_2$	1.1	6.9	2.39
3	XRD	$CaCl_2$	3.3	8	2.40
3	XRD	$CaCl_2$	5.2	8	2.40
4	XRD	$Ca(NO_3)_2$	3.6	7	2.44
4	XRD	$Ca(NO_3)_2$	6.0	7	2.45
5	XRD	$CaCl_2$	1.0	6	2.42
5	XRD	$CaCl_2$	2.0	6	2.42
5	XRD	$CaCl_2$	4.5	6	2.42
6	XRD	$CaCl_2$	2.0	6	2.46
6	XRD	$CaBr_2$	1.5	8	2.46
6	XRD	CaI_2	1.5	8	2.46
7	XRD+ND	$CaCl_2$	2.5	6.2(ND)	2.43–2.46(ND)
7	XRD+ND	$CaCl_2$	2.5	6.5(XRD)	2.43–2.46(XRD)
7	XRD+ND	$CaCl_2$	4.0	5.9(XRD)	2.43(XRD)
8	XRD	$CaCl_2$	1.0	8	2.45
9	ND	$CaCl_2$	4.5	5.5	2.41
10	ND	$CaCl_2$	1.0	10	2.46
10	ND	$CaCl_2$	2.8	7.2	2.39
10	ND	$CaCl_2$	4.5	6.4	2.40
11	ND	$CaCl_2$	6.4	6.95	2.41
11	ND	$CaCl_2$	4.0	7.3	2.40
12	EXAFS	$CaCl_2$	0.12	8	2.46
13	EXAFS	$CaCl_2$	0.2	6.8	2.43
13	EXAFS	$CaCl_2$	6.0	7.2	2.44

[a] The method, salt investigated, salt concentration (in molal units), and the resulting first-shell coordination number (CN) and average Ca−O distance (r[Ca−O]) are indicated.

and 4 m $CaCl_2$ solutions. At 2.5 m concentration they found consistent results of 6.5 ± 0.2 (XRD) and 6.2 ± 0.3 (ND) for the CN with a r[Ca−O] distance of 2.43–2.46 Å. At 4 m concentration the experiments suggested a CN of 5.9 ± 0.3 (XRD) with a r[Ca−O] distance of about 2.43 Å (XRD). Theoretical studies also contributed to the interpretation of experimental data and provided further (experimentally inaccessible) information on Ca^{2+} solvation (Table 2). The results also presented an important sensitivity to the applied methodology and parameters. Most empirical force field calculations relied on pairwise-additive interactions (no explicit electronic polarization). Molecular dynamics (MD) simulations with a modified central force–potential for water, together with ion–water and ion–ion pair potentials derived from ab initio calculations, suggested a first hydration shell consisting of either 9 or 10 water molecules and a r[Ca−O] distance of 2.49 Å for 1.1 m aqueous $CaCl_2$ solution.[14] In the higher concentration regime, CNs of 6.5 and 6.2 were suggested for 2.5 and 4.0 m $CaCl_2$, respectively,[7] together with a r[Ca−O] distance of 2.48 Å. Other simulations based on simple ab initio pair potentials gave CNs of 8–9.3 and r[Ca−O] distances of 2.39–2.54[2,15–19] in a similar concentration range. The use of empirical potentials including electron polarizability explicitly produced CNs between 7.2 and 10 and r[Ca−O] distances of 2.42–2.51 Å.[6,20,21] Monte Carlo (MC) simulations utilizing the MCHO potential form (including polarization) suggested values of 7 for the CN and 2.3 Å for the r[Ca−O].[22] The importance of electronic polarizability was investigated more directly in a comparison of classical simulations with pairwise additive versus explicitly polarizable ab initio derived ion–water potentials. The

Table 2. Theoretical Results on Ca^{2+} Solvation Previously Reported in the Literature from Monte Carlo (MC), Classical Molecular Dynamics (MD),[a] Quantum Mechanical/Molecular Mechanical (QM/MM) Simulations, Quantum Chemical Statistical Mechanical (QMSTAT) Calculations, and Car−Parrinello Molecular Dynamics (CPMD) Simulations[b]

ref	method	salt	concn (m)	CN	r[Ca−O] (Å)
2	MD	$CaCl_2$	1.1	9	2.39
6	MD-P(Åqvist)	Ca^{2+}		8	2.40
6	MD-P(Bounds)	Ca^{2+}		9–10	2.51
6	MD-P(Gromos)	Ca^{2+}		8	2.46
7	MD	$CaCl_2$	2.5	6.5	2.48
7	MD	$CaCl_2$	4.0	6.2	2.48
8	ab initio/MP2	Ca^{2+}	1	8	2.46
8	ab initio/MP2	Ca^{2+}	2.5	6.9	2.43
8	ab initio/MP2	Ca^{2+}	4	5.8	2.43
8	ab initio/MP2	Ca^{2+}	6	5.1	2.45
14	MD	$CaCl_2$	1.1	9–10	2.49
15, 16	MD-T	Ca^{2+}	∼1	7.1	2.50
15, 16	MD	Ca^{2+}	∼1	9.2	2.47
15, 16	QM/MM (ab initio)	Ca^{2+}	∼1	7.6	2.46
15, 16	QM/MM(DFT)	Ca^{2+}	∼1	8.1	2.51
17	MD	Ca^{2+}		8	2.50
18	MD	Ca^{2+}		9.3	2.54
19	QM/MM	Ca^{2+}	0.28	8.3	2.45
19	MD	Ca^{2+}	0.28	9.2	2.47
20	MD-P	Ca^{2+}		7.9	2.50
21	MD-P	Ca^{2+}		7.2–7.7	2.42–2.46
22	MC-P	Ca^{2+}		7	2.3
23	PCM/MD-P (PCM)	Ca^{2+}		8.6	2.50
27	QM/MM (ONIOM-XS)	Ca^{2+}		6	2.53
28	QMSTAT	Ca^{2+}		6.9	2.50
25	CPMD	Ca^{2+}		6	2.45
31	CPMD	Ca^{2+}		7–8	2.64
32	CPMD	Ca^{2+}		6.2	2.43
32	CPMD	Ca^{2+}		7	2.43
32	CPMD	Ca^{2+}		8	2.44
present study	CPMD	$CaCl_2$	1	6–7	2.39
present study	CPMD	$CaCl_2$	2	6	2.39
present study	CPMD	Ca^{2+}	2	6	2.39

[a] The "T", "P", or "PCM" added to the method indicates inclusion of three-body terms, explicit polarization, or polarizable continuum model implicit solvation. [b] The method, salt investigated, salt concentration (in molal units) and the resulting first-shell coordination number (CN) and average Ca−O distance (r[Ca−O]) are indicated.

nonpolarizable model resulted in a CN of 9.2 and r[Ca−O] distance of 2.47,[19] while variants of the polarizable one gave CNs ranging between 7.2 and 8.6 with r[Ca−O] distances between 2.42 and 2.50 Å.[21,23] A good method to assess the importance of including higher-order terms (three-body terms or explicit polarizability) in the expansion of the interaction potential is to perform ab initio calculations of small ion–water clusters, revealing differences in binding energy per additional water molecule upon increasing the cluster size.[24,25] Such ab initio molecular orbital calculations, performed at the restricted Hartree–Fock (HF) and second-order Møller–Plesset perturbation (MP2) levels of theory and followed by natural energy decomposition analysis, emphasized the importance of polarization effects in the binding energies of $M^{2+}(H_2O)_n$ clusters.[26] Polarization has also been recognized through classical MD calculations using the

polarizable continuum model (PCM) to be largely responsible for the nonclassical bent and pyramidal structures of the gas-phase di- and trihydrates and suggested to represent an important factor for determining the CN in solution.[23] Besides clusters in gas-phase, quantum-mechanical calculations also investigated solvation in the bulk. A comparison of (i) a classical simulation with a pairwise force field, (ii) a classical simulation with a force field including three-body terms, (iii) an ab initio quantum mechanical/molecular mechanical (QM/MM) simulation, and (iv) a density functional theory (DFT) QM/MM simulation reported CNs of 9.2, 7.1, 7.6, and 8.1, respectively,[15,16] with corresponding r[Ca−O] distances of 2.47, 2.50, 2.46, and 2.51 Å, respectively. QM/MM calculations with the ONIOM-XS (n-layered integrated molecular orbital and molecular mechanics extended to solvation) method led to a CN of 6 and an r[Ca−O] distance of 2.53 Å.[27] A CN of 6.9 together with an r[Ca−O] distance of 2.50 Å was also reported in a recent combined quantum chemical statistical mechanical (QMSTAT) calculation.[28] Finally, DFT based simulations using the Car–Parrinello molecular dynamics (CPMD) method[29,30] using different simulations protocols and density functionals (no counterions) showed variations in the water coordination number of Ca^{2+} from 6 to 8 and in the r[Ca−O] distance from 2.44 to 2.64 Å.[25,31,32]

An important point to keep in mind when performing classical or Car–Parrinello (CP) MD simulations to investigate the solvation properties of ions is that the finite size of the simulated systems and the approximate treatment of electrostatic interactions may have a significant impact on the simulation results.[33] In most cases, these simulations are performed under periodic boundary conditions (so as to eliminate surface effects) based on truly microscopic box volumes. When electrostatic interactions are handled as exactly periodic by application of lattice-sum methods (classical simulations) or plane-wave expansions (CP simulations), interactions between the reference box and its periodic images represent a significant (volume-dependent) perturbation compared to the ideal situation of a macroscopic solution at infinite dilution. Furthermore, in the case of non-neutral systems (e.g., single solvated ion without counterions), application of periodic electrostatics implicitly amounts to including a homogeneous neutralizing background charge density within the simulated box. The impact of periodicity induced artifacts on the solvation thermodynamics of ions is extremely large and cannot be neglected.[34–36] However, the associated structural perturbation (e.g., on pair distribution functions and CNs) may be more limited,[33,37] especially when the system is neutralized by the explicit inclusion of counterions. Nevertheless, the possible influence of artificially periodic electrostatics and neutralizing background charge on the results of previously reported CPMD simulations[25,31,32] of non-neutralized Ca^{2+} in water (which may still be important in view of the very small boxes considered in CP simulations compared to classical ones) has not been investigated systematically.

In the present study we expand on previously reported CPMD simulations.[25] The goal of this additional investigation is threefold: (i) comparing the results of a previous CPMD simulation[25] of 1 m Ca^{2+} in water (single Ca^{2+}, no counterions) with those of a new CPMD simulation of 1 m $CaCl_2$ (single Ca^{2+} and $2Cl^-$ counterions); (ii) evaluating via classical MD simulations the impact of the box size (via the homogeneous background charge density) on the simulated structural properties obtained from this previous CPMD simulation;[25] and (iii) investigating ion association properties in $CaCl_2$ solutions based on four new CPMD simulations of 2 m $CaCl_2$ ($2Ca^{2+}$ and $4Cl^-$) initiated from different starting configurations (free ions or Ca^{2+}-OH^--Ca^{2+}, Cl^--Ca^{2+}-Cl^- and Ca^{2+}-Cl^- species) along with one new CPMD simulation of 2 m Ca^{2+} ($2Ca^{2+}$; no counterions).

2. Computational Details

The CPMD[38] simulations were performed using the BLYP functional, i.e. with the exchange functional of Becke[39] and the correlation functional of Lee, Yang, and Parr,[40] using a Troullier-Martins norm-conserving pseudopotential for Ca^{2+} [41] and oxygen and hydrogen pseudopotentials as in ref 25. The mass of the hydrogen nucleus was set to that of the deuterium isotope. The valence electron wave function was expanded in plane waves with an energy cut off of 70 Ry. The fictitious electron mass was set to 600 au and the time step to 5 au (0.12 fs). The six simulations (see below) were carried out under periodic boundary conditions and involved 3 ps equilibration in the canonical ensemble, followed by 7.2 ps production in the microcanonical ensemble (the 1 m $CaCl_2$ production simulation was later extended to 19.2 ps). During the equilibration, the temperature was maintained at 320 K using a Nosé-Hoover thermostat.[42–45]

The systems consisted of a cubic box of 12.43 Å edge length, containing 58 water molecules (effective water density 1 $g.cm^{-3}$) and either 1 Ca^{2+} and 2 Cl^- ions (1 m $CaCl_2$) or $2Ca^{2+}$ and 4 Cl^- ions (2 m $CaCl_2$). A third system contained 62 water molecules, $2Ca^{2+}$ and no counterions (2 m Ca^{2+}). The resulting exact molalities and solution densities are 0.96 m and 1.00 $g.cm^{-3}$ (1 m $CaCl_2$), 1.91 m and 1.09 $g.cm^{-3}$ (2 m $CaCl_2$), and 1.79 m and 1.00 $g.cm^{-3}$ (2 m Ca^{2+}), respectively. Note that the electrostatic interactions are treated as exactly periodic (i.e., they include contributions from the interaction between nuclei and electrons within the computational box as well as interactions between this box and all its periodic copies). In the case of a non-neutral system (previous study[25] of 1 m Ca^{2+} and present simulation of 2 m Ca^{2+}), this implicitly involves the inclusion of a homogeneous neutralizing background charge density within the computational box. When the system is neutral (present simulations of 1 and 2 m $CaCl_2$), there is no such background charge.

The initial configuration for the 1 m $CaCl_2$ system was taken from a classical MD simulation using the ion–water potential of Floris et al.[23] and the extended simple point charge SPC/E water model.[46] This initial configuration contained seven water molecules in the first solvation shell of the ion. The simulations of the 2 m $CaCl_2$ system were initiated from four different configurations illustrated in Figure 1. The initial configuration of System A consisted of two six-coordinated Ca^{2+} ions at a distance of 4 Å (free

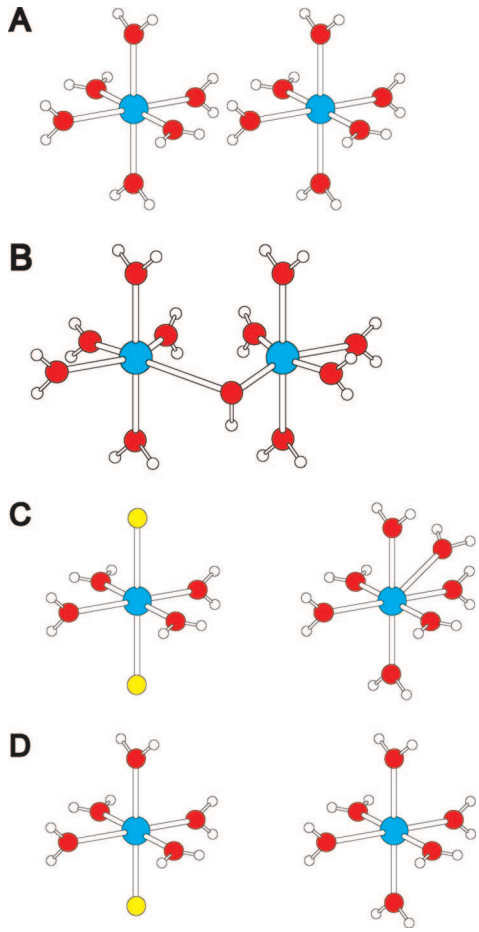

Figure 1. Initial configurations of the Car–Parrinello simulations (10.2 ps) of aqueous $CaCl_2$ ($2CaCl_2 + 58H_2O$; 2 m $CaCl_2$) corresponding to the simulated systems A−D (see Computational Details). A fifth system, System E, was also simulated in the absence of counterions ($2Ca^{2+} + 62H_2O$; 2 m Ca^{2+}). The corresponding initial configuration is identical to that of System A.

ions). The initial configuration of System B was generated from that of System A by slightly increasing the distance between the ions. This initial configuration consists of two six-coordinated Ca^{2+} ions at a distance of 4.5 Å, bridged by an OH^- group (species further noted Ca^{2+}-OH^--Ca^{2+}). The second hydrogen of the bridging water molecule formed an H_3O^+ ion in the bulk water. The initial configuration of System C was taken from a classical MD simulation using the ion–water potential of the GROMOS96 force field[47,48] and the SPC water model[46] Here, the Ca−Ca distance is 6.5 Å. While one of the Ca^{2+} ion is seven coordinated, the other forms axial Ca^{2+}-Cl^- bonds with two counterions, four water molecules being placed in equatorial positions (species further noted Cl^--Ca^{2+}-Cl^-). The initial configuration of System D was generated from that of System C by shortly increasing the distance between the Ca^{2+} and one Cl^- of the Cl^--Ca^{2+}-Cl^-species. This initial configuration consists of one six-coordinated ion (the seventh water having left the first coordination shell), the other ion forming one Ca^{2+}-Cl^- bond and presenting five water molecules in the first solvation shell (species further noted Ca^{2+}-Cl^-). Finally, a simulation was also performed for a System E containing $2Ca^{2+}$ ions (no Cl^-) and 62 water molecules. The initial structures of systems B−D were chosen in view of the role played by ion pairing (i.e., Ca^{2+}-Cl^-, Cl^--Ca^{2+}-Cl^-, and Ca^{2+}-H_2O-Cl^- species) in determining the thermodynamical properties of $CaCl_2$ solutions at high concentrations.[7,8,13,49] However, the Ca^{2+}-H_2O-Ca^{2+} species turned out to equilibrate to Ca^{2+}-OH^--Ca^{2+}.

The CPMD simulations were analyzed in terms of radial distribution functions (RDFs, $g(r)$), running coordination numbers (CNs, $n(r)$), time series of calcium−oxygen distances, and water dipole moment distribution in the first solvation shell. To examine the latter property, a localized molecular orbital analysis was performed by unitary transformation of Bloch orbitals to yield maximally localized Wannier functions.[50–52] Within the framework of the plane waves pseudopotential model, the maximally localized Wannier functions are analogous to the orbitals obtained by the Boys localization procedure commonly used in quantum chemistry.[53] The centroids of the Wannier functions (Wannier centers) were then used to define a dipole moment for individual water molecules in the simulations.

In addition to the CPMD simulations, a number of classical MD simulations were performed in order to evaluate the influence of modeling the counterion atmosphere implicitly by a homogeneous neutralizing background charge density in (CP or classical) simulations of Ca^{2+} under periodic boundary conditions (without explicit counterions). These simulations were performed at constant volume and temperature using the GROMOS96 program[47,48] together with the GROMOS 43a1 Ca^{2+} ion–solvent parameters and the SPC water model. The temperature was maintained close to 300 K by a Berendsen thermostat with a coupling time of 0.1 ps.[54] The systems involved one Ca^{2+} ion and a number of water molecules ranging from 8 to 150 in cubic boxes of edge lengths ranging from 6.48 to 16.59 Å (effective water density of about 1 $g.cm^{-3}$, omitting the ion). The electrostatic interactions were calculated using a lattice-sum method (P^3M,[55–57] with a sixth-order truncated-polynomial charge-shaping function of width 0.5 nm and a grid size of 32 × 32 × 32 points). This approach is the analog at the classical level of the periodic electrostatics used in the CPMD simulations. The cutoff radius for the van der Waals interactions was set to 10 Å. A multicell approach[58] was used to keep all parameters of the simulation constant when going to small simulation boxes (i.e., where the cutoff may exceed the half-box edge). The geometry of the water molecule was held rigid using SHAKE[47] with a relative geometric tolerance of 10^{-4}. A time step of 2 fs was used for integrating the equations of motion. All systems were equilibrated during 10 ps, followed by 500 ps production.

3. Results and Discussion

3.1. CPMD Simulations of a 1 m $CaCl_2$ Aqueous Solution. The Ca−O and Ca−H radial distribution functions (RDFs) as well as the running coordination numbers (CNs) obtained from the 7.2 ps CPMD simulation of a 1 m $CaCl_2$ solution at 320 K are displayed in Figure 2. The positions of the first maxima in the Ca−O and Ca−H RDFs are 2.39 Å and 3.03 Å, respectively, to be compared with correspond-

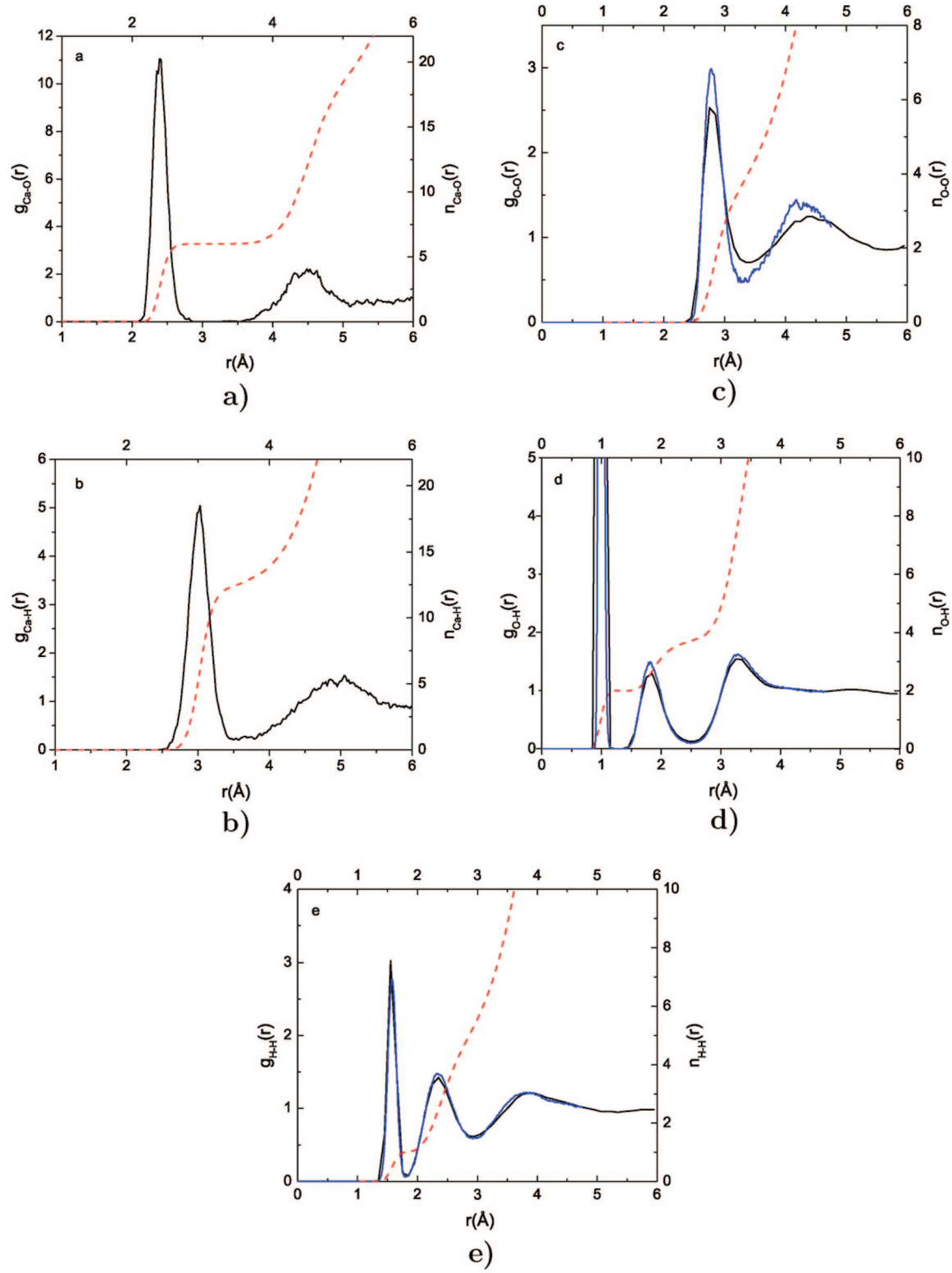

Figure 2. Radial distribution functions (RDFs; $g(r)$; black and blue lines) and running coordination numbers (CN, $n(r)$; dashed red lines) corresponding to calcium−water and water–water distances for the Car–Parrinello simulation (7.2 ps) of aqueous $CaCl_2$ (1 $CaCl_2$ + 58H_2O; 1 m $CaCl_2$; black and dashed red lines) and for Car–Parrinello simulations of pure water at the same level of theory (blue lines): a) Ca−O, b) Ca−H, c) O−O, d) O−H, e) H−H.

ing values of 2.45 Å and 2.98 Å for the previously reported CPMD simulation of 1 m Ca^{2+} without counterions.[25] For the Ca−O RDF the first and the second solvation shells are clearly separated by a region of nearly zero oxygen density, the two shells extending from about 2.1 to 2.8 Å and from about 3.5 to 5.1 Å, respectively. For the Ca−H RDF, the regions corresponding to the two solvation shells are broader, shifted to larger distances and partially overlapping. This difference between the two types of RDFs results from the preferential orientation of the water molecules (especially in the first shell) and the librational motions of the water molecules (especially in the second shell). Integrating the

Ca−O RDF over the first shell leads to an average first-shell CN of 6 (the corresponding integral over the Ca−H RDF is, as expected, about 12). Integrating the Ca−O RDF over the second shell leads to an average estimate of 13.2 water molecules. At 1 m $CaCl_2$ concentration the Cl^- counterions are found to systematically avoid the first and the second solvation shells of the Ca^{2+} ion (data not shown), so that their influence on the Ca^{2+} solvation structure is essentially negligible.

A comparison of the water–water O−O, O−H, and H−H RDFs with those obtained from CPMD simulation of pure water at the same level of theory[25] is also shown in Figure 2. The three functions evidence a loss of structure (particularly visible for the O−O RDF) in the regions corresponding to nearest and second nearest water molecules upon going from pure water to the $CaCl_2$ solution. The peaks corresponding to second nearest water molecules are also shifted to slightly larger distances. The first peaks in the O−O, O−H, and H−H RDFs are centered at 2.75, 0.95, and 1.55 Å, respectively (the former corresponding to intermolecular and the latter two to intramolecular distances).

The dipole moments of the six water molecules in the first coordination shell of Ca^{2+} were estimated based on the Wannier function approach as implemented in the CPMD code. This approach was previously applied[59] to calculate the dipole moment of the water molecule in the gas phase (1.86 D) and in the bulk (about 3 D). In aqueous $CaCl_2$ solutions, the dipole moment distribution for first-shell water molecules is shifted compared to that of pure water. It shows a maximum at 3.35 D, due to the electron polarization caused by the strong electric field of the ion. The same effect was also observed for Mg^{2+} and Be^{2+} ions in aqueous solution, with average first-shell water dipole moments of 3.3 and 3.1 D, respectively.[60,61]

The above results are very similar to those obtained in the previous investigation of a 1 m Ca^{2+} aqueous solution (no Cl^- counterions).[25] The counterions exert no noticeable effect on the first and second solvation shells of the Ca^{2+} ion (at the 1 m concentration considered here) and the first-shell CN remains six as found previously. This is also a first indication that the uniform neutralizing background charge density used in the CPMD simulation of the charged system[25] did not significantly affect the results (compared to the present explicit counterion treatment).

It has been suggested[21] that the low CNs and their sensitivity to the methodology employed in different CPMD simulations might be related to the fictitious electron mass used in these simulations.[25,31,32] We think that this is most likely not the case. The small mass of 600 au employed in this study produced the same results as in previous simulations (900 au fictitious electron mass in ref 25). In addition it has been convincingly shown[62,63] that no direct effect of the electron mass on static properties exists, if the masses employed stay within reasonable values and the simulations are correctly performed.

On the other hand, an important factor possibly affecting the CNs observed in different studies is the pseudopotential used to describe the core electrons of Ca^{2+}. Our tests show that it is important to include the $3p^6$ electronic state into the explicitly described valence electrons. A too soft Ca^{2+} ion results if these electrons are treated as part of the core. This has the effect that a larger water coordination shell can form and a CN of 7–8 is obtained.[31] Another important point is the choice of the exchange-correlation functional. Simulations utilizing the Perdew-Burke-Ernzerhof (PBE)[64] functional gave a CN of 6–7 for a flexible and 8 for a rigid model of water.[32] Recent calculations indicated that both PBE and BLYP exchange-correlation functionals produce too low water self-diffusion coefficients when compared to the experimental values.[65] In addition, it has been shown[66,67] that, at experimental density, both functionals lead to a very high pressure. Generalized gradient approximation density functionals, like BLYP and PBE, produce higher dipole moments when compared to dipole moments calculated with hybrid functionals. Furthermore, the isotropic polarizabilities are too large for most of these functionals. This is due to the well-known tendency of these density functionals to underestimate the HOMO–LUMO gap of molecular systems which, in turn, results in an overestimation of the molecular polarizability. Thus, the higher BLYP dipole moments and polarizabilities lead to lower CNs.

Another consequence of the overstructuring and slow diffusional dynamics of water when employing the BLYP representation is that only a few exchanges of molecules between the first and the second solvation shells are observed on the time scale of the present simulations. This feature is illustrated in Figure 3 (based on a trajectory extended to 19.2 ps). The initial configuration of the present simulation (pre-equilibrated using classical MD) presents seven water molecules in the first solvation shell of Ca^{2+}. The seventh water molecule leaves the shell shortly after the beginning of the simulation. The resulting six-coordinated Ca^{2+} structure remains stable until 13 ps and dominates the RDFs previously discussed (Figure 2; based on the initial 7.2 ps of the extended simulation). At this point, however, another water molecule enters the first solvation shell increasing again the CN to seven. Note that the seven-coordinated structures observed at the beginning and at the end of the simulation show more significant fluctuations in the first shell Ca−O distances (Figure 3) suggesting a destabilization of the solvation structure.

The results of the classical MD simulations, performed in order to investigate the box size dependence (via the background charge) of the structural properties in simulations of charged systems,[25] are reported in Table 3. Calculations with systems containing 8 to 150 water molecules and a single Ca^{2+} ion (no Cl^- counterion) have been performed at constant water density. The results show an effect on the coordination of Ca^{2+} for simulations with 50 water molecules or less, where the CN is observed to increase with the box size. This effect can be explained by the fact that the solvent molecules around the reference ion are perturbed by the periodic copies of the ion (undersolvation), the magnitude of the effect decreasing with increasing box size. An alternative (equivalent) interpretation is that the fraction of the homogeneous background charge that is inside the ionic volume (and thus reduces the field it exerts on the solvent) decreases upon increasing the box volume. The Ca−O

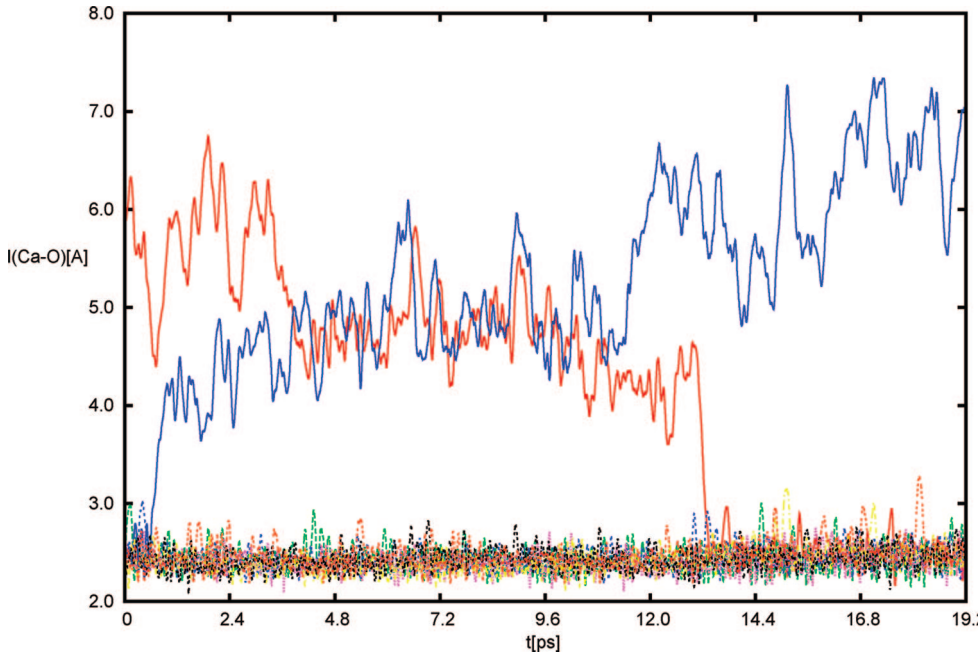

Figure 3. Time evolution of Ca−O distances along the Car–Parrinello simulation (19.2 ps; extended simulation) of aqueous $CaCl_2$ ($1CaCl_2 + 58H_2O$; 1 m $CaCl_2$). Only distances corresponding to the water molecules that belong to the first solvation shell at any time along the simulation are displayed.

Table 3. Coordination Number (CN) and First-Shell RDF Peak Position for the Ca−O Distance (r[Ca−O]) for Classical Simulations of Aqueous Ca^{2+} Solutions Involving 1 Ca^{2+} and the Indicated Number of Water Molecules[a]

H_2O	CN	r[Ca−O] (Å)
8	6.2	2.41
10	6.5	2.41
20	7.0	2.43
30	7.4	2.45
32	7.4	2.45
40	7.7	2.45
50	7.8	2.45
54	7.9	2.47
55	7.9	2.47
58	7.9	2.47
100	7.9	2.47
111	7.9	2.47
150	7.9	2.47

[a] At a constant effective water density of about 1 $g.cm^{-3}$, excluding the ion.

distance also increases along with the CN, due to the repulsion of the water molecules entering the first solvation shell. The same qualitative trend was found by Piquemal et al.[21] using a polarizable force field. In this study an increase of the CN from 7.2 to 7.7 was observed upon increasing the system size from 60 to 216 water molecules. However, this observation may also have other causes, the present results suggesting that finite-size effects on the solvation structure are essentially negligible above 50 water molecules.

3.2. CPMD Simulations of a 2 m $CaCl_2$ Aqueous Solution. The Ca−O and Ca−H RDFs as well as the running CNs obtained from the 7.2 ps CPMD simulations of a 2 m $CaCl_2$ (or Ca^{2+}) solution at 320 K are displayed in Figure 4 for the five different systems A−E. All systems remained close to the initial configuration during the entire simulation, and the final configurations of the runs were topologically identical to those displayed in Figure 1, justifying the calculation of average properties for the species considered (free ions, Ca^{2+}-OH^--Ca^{2+}, Cl^--Ca^{2+}-Cl^-, and Ca^{2+}-Cl^-) based on the different simulations. The positions of the first maxima in the Ca−O RDF range from 2.37 Å to 2.41 Å (to be compared with 2.39 Å for the simulation of 1 m $CaCl_2$, Figure 2, and 2.45 Å for the previous simulation[25] of 1 m Ca^{2+}). The first peaks corresponding to System A (2 m $CaCl_2$ solution) and System E (2 m Ca^{2+} solution; free ions) nearly exactly coincide, suggesting that the substitution of the chloride counterions by the uniform background charge density has little effect on first-shell solvation, at least when the two ions behave as independently solvated entities (i.e., at large enough distance). Note that System B has a slightly lower first peak and a second coordination shell shifted to smaller distances compared to System A. System C shows an even more pronounced decrease in the magnitude of the first peak along with a slightly altered curve shape for the second shell. Integrating the Ca−O RDFs up to the first minimum leads to average first-shell CNs ranging from 4 to 7 for the individual ions in the five different systems (Table 3). This number is about six for Systems A, B, and E. System C, representing the case of one seven-coordinated Ca^{2+} ion and another forming two Ca^{2+}-Cl^- bonds (d = 2.7–2.8 Å) and presenting four water molecules in equatorial positions, has the lowest RDF peak and an averaged CN of 5.5. The same averaged CN is also found for System D, but the RDF peak is higher and narrower, resulting from the smaller Ca−O distances compared to those of System C. The Ca−H radial distribution functions show the same trends (Figure 4, Table 3): almost no difference between Systems A, B, and E (CN of about 12 for the H atoms) and a reduced coordination for Systems C and D, due to the missing water molecules in the first solvation shell. The averaged dipole

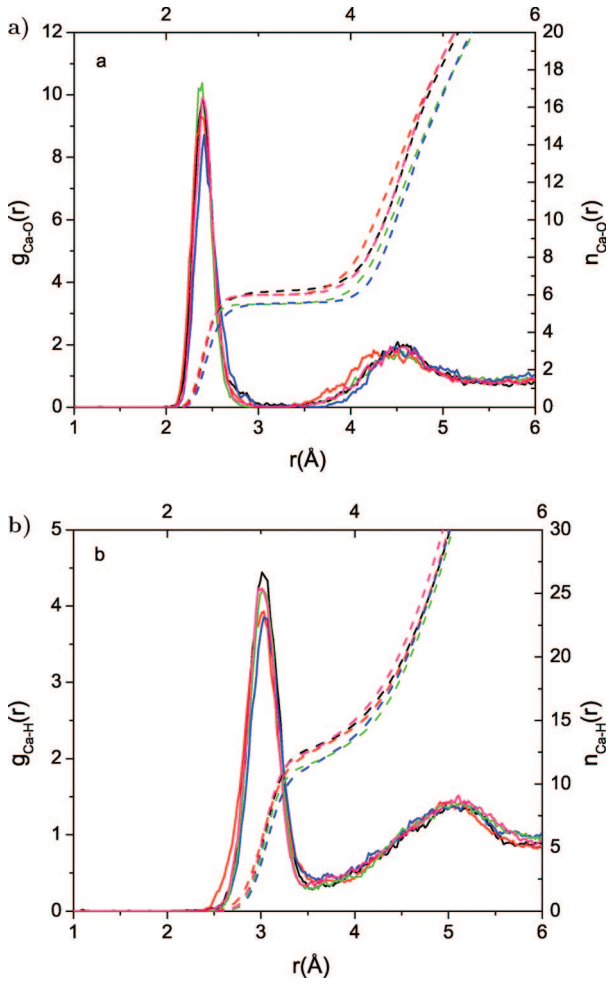

Figure 4. Radial distribution functions (RDFs; $g(r)$, solid lines) and running coordination numbers (CNs, $n(r)$, dashed lines) corresponding to Car–Parrinello simulations (7.2 ps) of aqueous $CaCl_2$ (Systems A−D; $2CaCl_2 + 58H_2O$; 2 m $CaCl_2$) or Ca^{2+} (System E; $2Ca^{2+} + 62H_2O$): a) Ca−O and b) Ca−H: System A (black), System B (red), System C (blue), System D (green), System E (pink), see Computational Details.

moment calculated for the water molecule in the first solvation shell are also reported in Table 3. The results show two trends: first, the higher the CN, the lower the dipole moment; second, the higher the concentration, the lower the dipole moment. A probable explanation is that at higher concentrations the Ca^{2+} hydration structure is weakened by the perturbation caused by the neighboring Ca^{2+} and Cl^- ions and the water polarization is reduced, resulting in lower dipole moments. A comparison of Systems A, C, and D with System E shows that even at 2 m concentration there is no significant influence of the chloride ions on the dipole moment distributions.

The structures of all systems (Figure 1) were preserved during the CPMD simulations. In System B, there was no water exchange between the first and the second shells, and the Ca^{2+}-OH^- distance remained at all times close to 2.39 Å. The coordination structure of the first ion in System C, involving two axial Ca^{2+}-Cl^- bonds and four water molecules in equatorial positions was also stable. However, the second ion was seven-coordinated, and the Ca−O distance oscillations were found to be larger (in analogy with Figure 3, although no exchange of water involving the first solvation shell was observed in this case).

Measurements on aqueous solutions of $MgCl_2$ and $CaCl_2$ showed an anomalous behavior of the osmotic coefficient for $CaCl_2$ (but not for $MgCl_2$) at about 5 m concentration.[49] This observation was suggested to result from the formation of Ca^{2+}-Cl^- species (contact ion pairs) at high concentrations. The formation of contact ion pairs has indeed been observed in high temperature aqueous solutions,[68–70] probably due to the reduced dielectric permittivity of water (leading to enhanced ion association). However, EXAFS studies suggested that Ca^{2+}-OH_2-Cl^- species (solvent separated ion pairs) rather than contact ion pairs were responsible for the anomaly of the osmotic coefficient at 5 m concentration.[13] Different molal concentrations appear to result in the dominance of different species: solvent separated pairs at 6 m concentration and contact pairs at 9.2 m concentration.[13] Average Ca−O distances were estimated to be 2.44 Å, and average Ca−H distances to be 2.97 Å.[13] Independent ND experiments[11] confirmed many of the findings of this EXAFS study.[13] Specifically: minimal changes in the nearest-neighbor Ca−O correlation, a mean CN of about 7 for the first hydration shell, and the absence of significant Ca^{2+}-Cl^- contact ion pairing even at concentrations as high as 6.4 m.[11] Chloride ions were proposed to be in the second coordination shell (Ca^{2+} to Cl^- distances of 4.6–5.6 Å) with the dominance of Ca^{2+}-OH_2-Cl^- solvent-separated pairs at 4 and 6.4 m. XRD experiments also suggested the dominance of these species at 1 m and the simultaneous presence of both Ca^{2+}-OH_2-Cl^- (solvent separated) and Ca^{2+}-Cl^- (contact) ion pairs at 4 and 6 m.[8] XRD experiments reported first-shell Ca−O distances in the range 2.43–2.46 Å, Ca^{2+}-Cl^- distances of about 2.75 Å and a Cl^--O distance of about 3.25 Å at 4–6 m.[8] Recently, Megyes et al.[7] performed XRD, ND, and MD studies and discussed the relative abilities of these methods to detect the ion pair formation. They point out that XRD could detect ion pairs in the case of concentrated solutions (more than 4 m), while ND required very careful isotope substitution in order to be able to detect ion pairs in solution. The MD results were in general accordance with the XRD experimental findings.[7]

The present study suggests that the Ca^{2+}-Cl^- (contact) or Ca^{2+}-H_2O−Cl^- (solvent separated) ion pairs may be present even at lower concentrations (2 m), at least as transient species stable on the 10 ps time scale probed by the present simulations. However, their relative stabilities (i.e., equilibrium concentrations) cannot be evaluated based on such short simulations. In addition, a particularly interesting result is the observation of a Ca^{2+}-OH^--Ca^{2+} solvent-separated species, instead of the Ca^{2+}-H_2O-Ca^{2+} species. To the best of our knowledge, XRD, EXAFS, and ND experiments show no evidence for such a hydroxyl-separated ion pair. To rationalize System B, we looked at the thermodynamics of formation, deprotonation, and charge reduction of the hydrates of doubly charged ions. One of the methods to produce doubly charged metal ion hydrates is the clustering method. This method is based on a charge reduction, which can be viewed as a proton transfer reaction, i.e. $M(H_2O)^{2+} + H_2O \rightarrow M(OH)^+ + H_3O^+$ in the gas phase (M: divalent

metal ion). Density functional theory cluster calculations have shown that in the case of Ca^{2+}, the charge reduction reaction costs only 19.2 kcal/mol, while the competing reaction of water loss would require 48.1 kcal/mol.[71] Moreover, it has been proposed that water, with a proton affinity of 165 kcal/mol, is able to deprotonate $Ca(H_2O)^{2+}$. Because of the large release of kinetic energy associated with the Coulombic repulsion between the two positively charged ions produced by the charge reduction reaction, only bases whose proton affinity is significantly larger than the proton affinity of $CaOH^+$ (108 kcal/mol) will be able to induce a proton transfer.[72] A similar situation arises for the Al^{3+} ion where the kinetics of proton and water exchange in aqueous Al^{3+} support five-coordinated $Al(H_2O)_4OH^{2+}$ ions as the predominant form of $AlOH(aq)^{2+}$ under ambient conditions.[73]

4. Conclusions

In the present study, six CPMD simulations of aqueous $CaCl_2$ and Ca^{2+} solutions are reported.

The results of the simulation of a 1 m $CaCl_2$ solution ($1CaCl_2 + 58H_2O$) are consistent with those of a previous calculation on a 1 m Ca^{2+} solution ($1Ca^{2+} + 54H_2O$) using the same methodology.[25] Classical MD simulations of a single Ca^{2+} ion in boxes of increasing sizes confirm that beyond about 50 water molecules included in the computational box, the calculated structural properties (RDF peaks and CN) become essentially independent of the box size. The previous and present CPMD simulations support a first shell RDF peak for the Ca−O distance at 2.39 Å and a CN of 6 for the first solvation shell at a concentration of 1 m. However, the time frame of the simulations (about 10 ps) does not allow for a statistical sampling of water exchange between first and second solvation shells, and it is likely that the converged averaged CN using the present methodology would be slightly larger than 6. The second solvation shell of Ca^{2+} ranges from about 3.5 to 5.1 Å, and encompasses about 13.2 water molecules on average. Localized orbital analysis based on Wannier functions calculations shows a polarization of water molecules in the first solvation shell, which results in an increased dipole moment of 3.3 D compared to that of the bulk water (about 3 D). The tests performed in the present study thus indicate that there are no artifacts from simulation protocols using uniform background charges and artificial periodicity at the experimental concentration of 1 m. In former studies only the stability of the results toward infinite dilution was considered. The present results achieved with more strict parameters used in the Car–Parrinello simulations give more credit to previous simulations.[25,32]

Simulations of a 2 m $CaCl_2$ solution ($2CaCl_2 + 58H_2O$) or of a 2 m Ca^{2+} solution ($2Ca^{2+} + 62H_2O$) starting from free (i.e., widely separated) ions also produced very similar results (among each other and compared to the 1 m case). Recent combined XRD and ND experiments[7] suggest CN of 6.5 ± 0.2 and 6.2 ± 0.3 together with an average Ca−O distance between 2.43 and 2.46 Å for 2.5 m solutions, respectively. The slightly too low values for these quantities in our simulations are most likely due to shortcomings in the functional (BLYP) employed and not due to simulation protocol parameters or system size dependencies, as was recently[21] suggested. Another source of discrepancies might be that simulations performed at the experimental density result in an effectively overpressurized sample when using the BLYP functional. Finally, the simulations at 2 m $CaCl_2$ solutions ($2CaCl_2 + 58H_2O$) starting from four different configurations support the stability of Ca^{2+}-Cl^- (contact) and Ca^{2+}-OH_2-Cl^- (solvent-separated) ion pairs on the 10 ps time scale. This result is in agreement with recent XRD[8] and EXAFS[13] experiments. The solvent-separated cation pair was found to be present in the simulations in its deprotonated form Ca^{2+}-OH^--Ca^{2+}. To the best of our knowledge, no such specie has been reported or suggested based on experiment. Although the above species were found to be stable on the 10 ps time scale, it is impossible to infer their relative stability (i.e., their equilibrium concentrations) from the present simulations. However, the simulations suggest that at higher concentrations, a wider variety of species may exist, and the study of these complex solutions by computational means makes the explicit inclusion of electronic structure necessary. On the other hand, is it also clear from our simulations that the scope of such first principles simulations is limited due to the restricted time frame currently available.

Table 4. First-Shell Coordination Number (CN), First-Shell RDF Peak Position for the Ca−O and Ca−H Distances (r[Ca−O] and r[Ca−H]), and Average Dipole Moments of First-Shell Water Molecules for Car−Parrinello Simulations of Different Aqueous Ca^{2+} or $CaCl_2$ Solutions

system	atom	CN	r[Ca−O] (Å)	r[Ca−H] (Å)	dipole (D)
$Ca + 54H_2O$	Ca_1	6	2.45	2.98	3.40
$CaCl_2 + 58H_2O$	Ca_1	6(7)	2.39	3.03	3.35
A	Ca_1	6	2.39	3.01	3.25
A	Ca_2	6	2.39	3.01	3.25
B	Ca_1-Ca_2	12	2.37	3.03	3.15
C	Ca_1	7	2.41	3.03	3.15
C	Ca_2	4	2.41	3.03	3.25
D	Ca_1	6	2.39	3.03	3.20
D	Ca_2	5	2.39	3.03	3.25
E	Ca_1	6	2.39	2.97	3.25
E	Ca_2	6	2.39	2.97	3.25

Acknowledgment. T.T. wants to thank Dr. A. P. Seitsonen and Dr. M. Iannuzzi for fruitful discussions. Calculations were performed on the Matterhorn Cluster at the University of Zürich.

References

(1) da Silva, J. F.; Williams, R. *The Biological Chemistry of the Elements*; Clarendon Press: Oxford, 1991; pp 278–314.

(2) Probst, M.; Radnai, T.; Heinzinger, K.; Bopp, P.; Rode, B. J. *Phys. Chem.* **1985**, *89*, 753–759.

(3) Albright, J. J. *Chem. Phys.* **1972**, *1972*, 3783.

(4) Smirnov, P.; Yamagami, M.; Wakita, H.; Yamaguchi, T. *J. Mol. Liq.* **1997**, *73–4*, 305–316.

(5) Licheri, G.; Piccaluga, G.; Pinna, G. J. *Chem. Phys.* **1976**, *64*, 2437–2441.

(6) Jalilehvand, F.; Spangberg, D.; Lindqvist-Reis, P.; Hermansson, K.; Persson, I.; Sandstrom, M. *J. Am. Chem. Soc.* **2001**, *123*, 431–441.

(7) Megyes, T.; Bakó, I.; Bálint, S.; Grósz, T.; Radnai, T. J. *Mol. Liq.* **2006**, *129*, 63–74.

(8) Megyes, T.; Grósz, T.; Radnai, T.; Bakó, I.; Pálinkás, G. J. *Phys. Chem. A* **2004**, *108*, 7261–7271.

(9) Cummings, S.; Enderby, J.; Howe, R. J. *Phys. C: Solid State Phys.* **1980**, *13*, 1–8.

(10) Hewish, N.; Neilson, G.; Enderby, J. *Nature* **1982**, *297*, 138–139.

(11) Badyal, Y.; Barnes, A.; Cuello, G.; Simonson, J. J. *Phys. Chem. A* **2004**, *108*, 11819–11827.

(12) Spangberg, D.; Hermansson, K.; Lindqvist-Reis, P.; Jalilehvand, F.; Sandstrom, M.; Persson, I. J. *Phys. Chem. B* **2000**, *104*, 10467–10472.

(13) Fulton, J.; Heald, S.; Badyal, Y.; Simonson, J. J. *Phys. Chem. A* **2003**, *107*, 4688–4696.

(14) Pálinkás, G. *Chem. Phys. Lett.* **1986**, *126*, 251–254.

(15) Schwenk, C.; Loeffler, H.; Rode, B. J. *Chem. Phys.* **2001**, *115*, 10808–10813.

(16) Schwenk, C.; Rode, B. *Pure Appl. Chem.* **2004**, *76*, 37–47.

(17) Obst, S.; Bradaczek, H. J. *Phys. Chem.* **1996**, *100*, 15677–15687.

(18) Periole, X.; Allouche, D.; Daudey, J.; Sanejouand, Y. J. *Phys. Chem. B* **1997**, *101*, 5018–5025.

(19) Tongraar, A.; Liedl, K.; Rode, B. J. *Phys. Chem. A* **1997**, *101*, 6299–6309.

(20) Kalko, S.; Sesé, G.; Padró, J. J. *Chem. Phys.* **1996**, *104*, 9578–9585.

(21) Piquemal, J.; Perera, L.; Cisneros, G.; Ren, R.; Pedersen, L.; Darden, T. J. *Chem. Phys.* **2006**, *125*, 054511.

(22) Bernal-Uruchurtu, M.; Ortega-Blake, I. J. *Chem. Phys.* **1995**, *103*, 1588–1598.

(23) Floris, F.; Persico, M.; Tani, A.; Tomasi, J. *Chem. Phys. Lett.* **1994**, *227*, 126–132.

(24) Pavlov, M.; Siegbahn, P.; Sandstrom, M. J. *Phys. Chem. A* **1998**, *102*, 219–228.

(25) Bakó, I.; Hutter, J.; Pálinkás, G. J. *Chem. Phys.* **2002**, *117*, 9838–9843.

(26) Glendening, E.; Feller, D. J. *Phys. Chem.* **1996**, *100*, 4790–4797.

(27) Kerdcharoen, T.; Morokuma, K. J. *Chem. Phys.* **2003**, *118*, 8856–8862.

(28) Tofteberg, T.; Ohrn, A.; Karlstrom, G. *Chem. Phys. Lett.* **2006**, *429*, 436–439.

(29) Car, R.; Parrinello, M. *Phys. Rev. Lett.* **1985**, *55*, 2471–2474.

(30) Marx, D.; Hutter, J. In *Modern Methods and Algorithms of Quantum Chemistry*; Grotendorst, J., Ed.; FZ Jülich: Germany, 2000; Vol. 1 of NIC Series, pp 329–477.

(31) Naor, M. M.; Nostrand, K. V.; Dellago, C. *Chem. Phys. Lett.* **2003**, *369*, 159–164.

(32) Lightstone, F. C.; Schwegler, E.; Allesch, M.; Gygi, F.; Galli, G. *ChemPhysChem* **2005**, *6*, 1745–1749.

(33) Hünenberger, P. H.; McCammon, J. A. J. *Chem. Phys.* **1999**, *110*, 1856–1872.

(34) Kastenholz, M.; Hünenberger, P. H. J. *Phys. Chem. B* **2004**, *108*, 774–788.

(35) Kastenholz, M.; Hünenberger, P. H. J. *Chem. Phys.* **2006**, *124,* 124106.

(36) Kastenholz, M.; Hünenberger, P. H. J. *Chem. Phys.* **2006**, *124*, 224501.

(37) Peter, C.; van Gunsteren, W. F.; Hünenberger, P. H. J. *Chem. Phys.* **2002**, *116*, 7434–7451.

(38) *CPMD V3.11*; copyright IBM Corp 1990–2007, copyright MPI für Festkörperforschung Stuttgart 1997–2001.

(39) Becke, A. D. *Phys. Rev. A* **1988**, *38*, 3098–3100.

(40) Lee, C.; Yang, W.; Parr, R. G. *Phys. Rev. B* **1988**, *37*, 785–789.

(41) Troullier, N.; Martins, J. L. *Phys. Rev. B* **1991**, *43*, 1993–2006.

(42) Nosé, S. J. *Chem. Phys.* **1984**, *81*, 511–519.

(43) Nosé, S. *Mol. Phys.* **1984**, *52*, 255–268.

(44) Hoover, W. G. *Phys. Rev. A* **1985**, *31*, 1695–1697.

(45) Martyna, G. J.; Klein, M. L.; Tuckerman, M. E. J. *Chem. Phys.* **1992**, *97*, 2635–2643.

(46) Berendsen, H. J. C.; Grigera, H. J. C.; Straatsma, T. P. J. *Chem. Phys.* **1987**, *91*, 6269–6271.

(47) van Gunsteren, W.; Billeter, S.; Eising, A.; Hünenberger, P.; Krüger, P.; Mark, A.; Scott, W.; Tironi, I. *Biomolecular Simulation: The GROMOS96 Manual and User Guide*; Hochschulverlag an der ETH Zurich/Biomos: Zurich/Groningen, 1996.

(48) Scott, W. R. P.; Hünenberger, P. H.; Tironi, I. G.; Billeter, A. E. M. S. R.; Fennen, J.; Torda, A. E.; Huber, T.; Krüger, P.; van Gunsteren, W. F. J. *Phys. Chem. A* **1999**, *103*, 3596–3607.

(49) Phutela, R.; Pitzer, K. J. *Solut. Chem.* **1983**, *12*, 201–207.

(50) Marzari, N.; Vanderbilt, D. *Phys. Rev. B* **1997**, *56*, 12847–12865.

(51) Berghold, G.; Mundy, C. J.; Romero, A. H.; Hutter, J.; Parrinello, M. *Phys. Rev. B* **2000**, *61*, 10040–10048.

(52) Kirchner, B.; Hutter, J. J. *Chem. Phys.* **2004**, *121*, 5133–5142.

(53) Boys, S. F. *Rev. Mod. Phys.* **1960**, *32*, 296–299.

(54) Berendsen, H. J. C.; Postma, J. P. M.; van Gunsteren, W. F.; DiNola, A.; Haak, J. R. J. *Chem. Phys.* **1984**, *81*, 3684–3690.

(55) Hockney, R. W.; Eastwood, J. W. *Computer simulation using particles.* Institute of Physics Publishing: Bristol, 1981; pp 267–304.

(56) Hünenberger, P. H. Lattice-sum methods for computing electrostatic interactions in molecular simulations. In *Simulation and theory of electrostatic interactions in solution: Computational chemistry, biophysics, and aqueous solutions*. Pratt, L. R., Hummerand, G., Eds.; American Institute of Physics: New York, U.S.A., 1999; pp 17–83.

(57) Hünenberger, P. H. J. *Chem. Phys.* **2000**, *113*, 10464–10476.

(58) de Vries, A. H.; Chandrasekhar, I.; van Gunsteren, W. F.; Hünenberger, P. H. J. *Phys. Chem. B* **2005**, *109*, 11643–11652.

(59) Silvestrelli, P. L.; Parrinello, M. J. *Chem. Phys.* **1999**, *111*, 3572–3580.

(60) Lightstone, F. C.; Schwegler, E.; Hood, R. Q.; Gygi, F.; Galli, G. *Chem. Phys. Lett.* **2001**, *343*, 549–555.

(61) Marx, D.; Sprik, M.; Parrinello, M. *Chem. Phys. Lett.* **1997**, *273*, 360–366.

(62) Kuo, I.-F. W.; Mundy, C. J.; McGrath, M. J.; Siepmann, J. I.; VandeVondele, J.; Sprik, M.; Hutter, J.; Chen, B.; Klein, M. L.; Mohamed, F.; Krack, M.; Parrinello, M. *J. Phys. Chem. B* **2004**, *108*, 12990–12998.

(63) Kuo, I.-F. W.; Mundy, C. J.; McGrath, M. J.; Siepmann, J. I. *J. Chem. Theory Comput.* **2006**, *2*, 1274–1281.

(64) Perdew, J. P.; Burke, K.; Ernzerhof, M. *Phys. Rev. Lett.* **1996**, *77*, 3865–3868.

(65) Todorova, T.; Seitsonen, A. P.; Hutter, J.; Kuo, I.-F. W.; Mundy, C. J. J. *Phys. Chem. B* **2006**, *110*, 3685–3691.

(66) McGrath, M. J.; Siepmann, J. I.; Kuo, I.-F. W.; Mundy, C. J.; VandeVondele, J.; Hutter, J.; Mohamed, F.; Krack, M. *J. Phys. Chem. A* **2006**, *110*, 640–646.

(67) McGrath, M. J.; Siepmann, J. I.; Kuo, I.-F. W.; Mundy, C. J. *Mol. Phys.* **2006**, *104*, 3619–3626.

(68) Hoffmann, M.; Darab, J.; Palmer, B.; Fulton, J. J. *Phys. Chem. A* **1999**, *103*, 8471–8482.

(69) de Bakker, P. I. W.; Hünenberger, P. H.; McCammon, J. A. J. *Mol. Biol.* **1999**, *285*, 1811–1830.

(70) Peric, L.; Pereira, C. S.; Hünenberger, P. H. *Mol. Simul.* **2007**, submitted for publication.

(71) Peschke, M.; Blades, A.; Kebarle, P. *Int. J. Mass Spectrom.* **1999**, *187*, 685–699.

(72) Gronert, S. J. *Am. Chem. Soc.* **1996**, *118*, 3525–3526.

(73) Swaddle, T. W.; Rosenqvist, J.; Yu, P.; Bylaska, E.; Phillips, B. L.; Casey, W. H. *Science* **2005**, *308*, 1450–1453.

CT700302M